Available online at website: https://journal.bcrec.id/index.php/bcrec

Bulletin of Chemical Reaction Engineering & Catalysis, 19 (1) 2024, 126-133

Research Article

Catalytic Hydroconversion of Lauric Acid Over Poly(N-vinyl-2-pyrrolidone)-Coated Pd Nanoparticles on ZIF-8

Deliana Dahnum[1,*], Holanda Ramadhita[2], A. Andreas[1], Joni Prasetyo[1], Aditia Nur Bakti[3], Huyen Tran Dang[4]

[1]Research Center for Chemistry, National Research and Innovation Agency Republic of Indonesia (BRIN), Indonesia.
[2]Department of Renewable Energy Engineering, Prasetiya Mulya University, Indonesia.
[3]Research Center for Testing Technology and Standards, National Research and Innovation Agency Republic of Indonesia (BRIN), Indonesia.
[4]Chemical Process Technology Division, Korea Research Institute of Chemical Technology, Republic of Korea.

Received: 5th January 2024; Revised: 12th February 2024; Accepted: 13th February 2024
Available online: 14th February 2024; Published regularly: April 2024

Abstract

A subclass of Metal-Organic Frameworks, Zeolitic Imidazole Frameworks-8 (ZIF-8) is known as an emerging material that has the characteristic of a large surface area, good thermal stability as well as a high porosity. Instead of having extraordinary properties, ZIF-8 consists of Lewis acid and Lewis base site on its Zn metals and 2-methylimidazole which are the important components for the catalyst. In this study, Pd-Poly(N-vinyl-2-pyrrolidone) coated on ZIF-8 (Pd-PVP@ZIF-8) was synthesized by mixed Pd-PVP solution and ZIF-8 precursors at room temperature. The Pd-PVP solution was varied from 10 to 50 ml to differentiate the Pd concentration in ZIF-8. As-synthesized 50 ml of Pd-PVP on ZIF-8 (50Pd-PVP@ZIF-8) showed catalytic activity in the conversion of 98.6% lauric acid to produce 78.2% of 1-dodecanol at optimum condition 320 °C for 6 h. The synergy between Pd-PVP as metal and ZIF-8 as metal support as well as high dispersion of Pd particles could enhance performance in the conversion of lauric acid.

Keywords: Pd-PVP@ZIF-8; catalyst; hydroconversion; lauric acid

How to Cite: D. Dahnum, H. Ramadhita, A. Andreas, J. Prasetyo, A.N. Bakti, H.T. Dang (2024). Catalytic Hydroconversion of Lauric Acid Over Poly(N-vinyl-2-pyrrolidone)-Coated Pd Nanoparticles on ZIF-8. *Bulletin of Chemical Reaction Engineering & Catalysis*, 19 (1), 126-133 (doi: 10.9767/bcrec.20114)

Permalink/DOI: https://doi.org/10.9767/bcrec.20114

1. Introduction

Biomass as a renewable material has attracted lots of interest worldwide because of its abundance, renewability, and potential to reduce greenhouse gas (GHG) emissions [1]. Biomass, including fatty acid, stands out for its ability to replace fossil fuels that have caused many serious environmental problems, such as climate change and global warming. The production of chemicals and fuels has gained interest in the context of the up-grading of bio-based feedstock to valuable materials.

Fatty acids can be converted to fatty alcohols, which are basic building blocks in industries such as cosmetics, lubricants, surfactants, plasticizers, and fuel [2]. The hydrogenation reaction can be proceeded to produce fatty alcohols. However, the side reactions including decarboxylation and decarbonylation to less carbon alkene, hydrogenolysis of the produced alcohol to alkanes, and the esterification of the produced alcohol decreased the selectivity of the product [3,4].

The catalyst plays an important role in the reaction. Designing metal-based and support catalysts with good physicochemical properties can affect the selectivity toward desired products and prevent side reactions [5]. It was reported a precious catalyst, such as Pt [6], Rh [7], Ru [8], or Re [9], to be active to convert fatty acid to fatty alcohol. Moreover, the noble metal Pd-nps supported on $CuZnAl_2O_3$ showed activity to

---

* Corresponding Author.
Email: deli001@brin.go.id (D. Dahnum);

convert 80.5% of methyl decanoate to decanol at 80.3% yield [10]. Re–Pd bimetallic catalysts supported on silica also was found to be effective for selective hydrogenation of stearic acid to stearyl alcohol due to the Pd plays a role in promoting the reduction and dispersion of Re ion [9]. In addition, the catalyst support also contributes to enhancing the catalytic activity of the reaction. As reported recently, Ni-Fe/SiO_2-ZrO_2 was a selective catalyst due to the synergy of SiO_2-ZrO_2 which provides a scarce oxygen vacancy supporting lewis acid Ni-Fe to produce oleic acid to fatty alcohol [11]. In other silica-based catalysts, ReOx–Pd/SiO_2 was reported as a selective hydrogenation catalyst over fatty alcohols in which cooperation of ReOx species, Pd metal particles, and catalyst support silica enhanced the activity and suppressed side reaction [9].

Metal-organic framework (MOF) is a new type of support material with high surface area, narrow pore distribution, and porosity. A high surface area with narrow pore distribution enables the uniform distribution of active metal nanoparticles, resulting in better catalytic activity and selectivity control [12]. ZIF-8, as a member of MOF material that is composed of Zn^{2+} ions coordinating with the N atom of the imidazolate (IM) ligand, has the characteristics of large surface area, good thermal stability, and high porosity, which has shown great potential for deoxygenation reaction [13]. Noble metals such as Pd have been extensively applied as a catalyst for deoxygenation as a consequence of high activity to dissociate H_2, decreasing the energy barriers in C−O/C−C bond cleavages [14]. The synthesis of ZIF-8 as a support catalyst for monometallic or bimetallic nanoparticles has been widely investigated because it can improve the catalytic activity and selectivity. Jing *et al.* [15] reported NiO-PTA/ZIF-8 catalyst increased the selectivity of C_{15} – C_{18} by over 36% compared with NiO-PTA/Al_2O_3 and the catalytic efficiency resulted in better 10 times by using NiO-PTA/ZIF-8 rather than NiO-PTA/Al_2O_3, due to its large surface area supported with ZIF micropore structure.

Herein, we synthesized ZIF-8 coated with poly(N-vinyl-2-pyrrolidone) (PVP), (denoted as Pd-PVP@ZIF-8) and used it as a catalyst for hydroconversion of lauric acid to lauryl alcohol (1-dodecanol). To the best of our knowledge, the report of using ZIF-8 as a support of the Pd-nanoparticles for hydroconversion of fatty acid to fatty alcohol has not been reported. The catalytic activity of Pd-PVP@ZIF-8 was investigated in a high-pressure reactor under a certain temperature and time. The synthesized catalysts were characterized by X-ray Diffraction (XRD), Fourier Transform-Infrared Spectra (FT-IR), Brunauer-Emmett-Teller (BET), Scanning Electron Microscopy (SEM), and Transmission Electron Microscopy (TEM).

2. Materials and Method

2.1 Chemicals

All chemicals used in this study were of analytical grade, commercially available, and were used without further purification. Zinc nitrate hexahydrate, 2-methylimidazole, $Pd(OAc)_2$, diethylamine, polyvinylpyrrolidone (PVP), lauric acid, and methanol were purchased from Sigma-Aldrich.

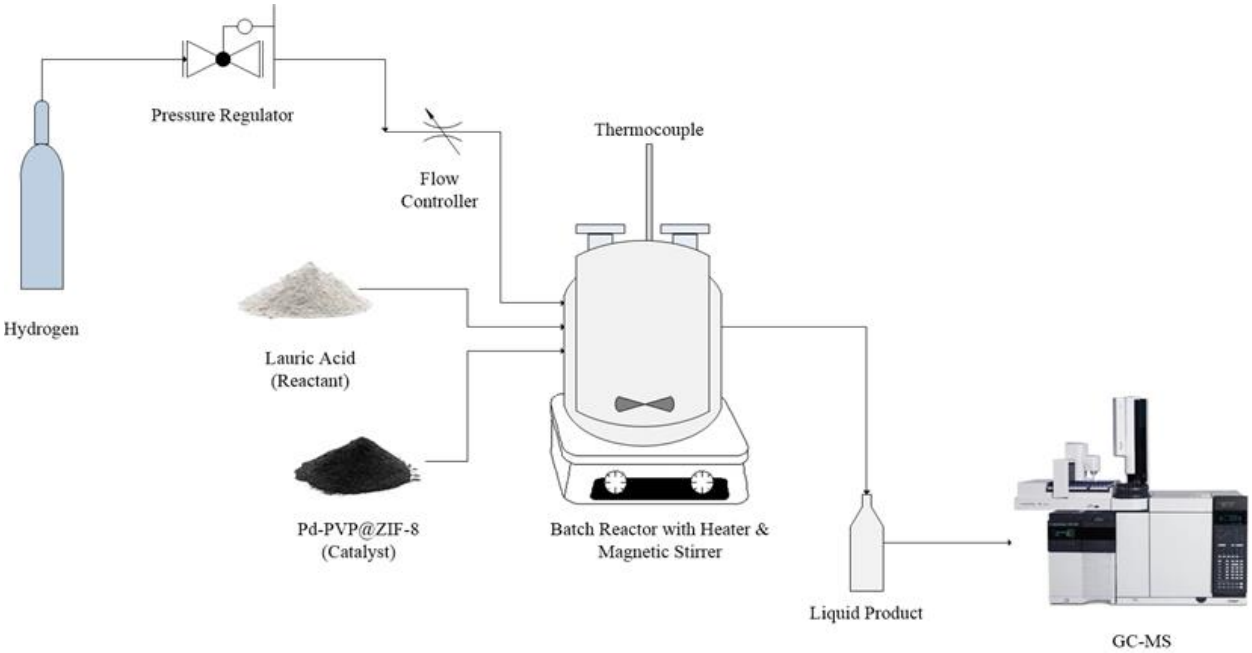

Figure 1. Experimental setup for testing the catalyst performance.

2.2 Synthesis of Pd-PVP@ZIF-8

The Pd-PVP@ZIF-8 was prepared by the methanolic reduction method as reported previously with a slight modification [16]. Firstly, the Pd-PVP solution was prepared by mixing 0.1132 g of $Pd(OAc)_2$ and 10 g of PVP in 100 mL of methanol, and the solution was stirred at 60 °C under reflux conditions. After 3 h, the solution was cooling down to room temperature. The Pd-PVP@ZIF-8 was synthesized by mixing 2 g (6.7 mmol) $Zn(NO_3)_2.6H_2O$, 1.10 g (13.4 mmol) of 2-Methylimidazole, 10 ml of diethylamine, 200 mL of methanol, and PVP-Pd solution for each of 10, 20, 30, and 50 mL. The mixture was stirred at room temperature for 48 h. The precipitated solid was then separated by centrifuge and washed several times with methanol. After dried at 150 °C, Pd-PVP@ZIF-8 was collected and denoted as 10Pd-PVP@ZIF-8, 20Pd-PVP@ZIF-8, 30Pd-PVP@ZIF-8, 50Pd-PVP@ZIF-8, respectively for the addition of 10 ml, 20 ml, 30 ml, and 50 ml of Pd-PVP solution.

Pure ZIF-8 was synthesized to confirm the formation of ZIF-8 in the synthesized materials. Around 4 g (13.4 mmol) of $Zn(NO_3)_2.6H_2O$ and 2.2 g (26.8 mmol) 2-Methylimidazole were mixed in the 200 ml of methanol with the addition of 20 g of diethylamine. The mixture was stirred at room temperature. After 48 h, the precipitate was isolated from the solution using a centrifuge. The formed solid ZIF-8 was dried at 130 °C for 3 h under oven vacuum.

2.3 Catalytic Performance

The catalytic reaction was conducted in a high-pressure reactor equipped with a heater and magnetic stirrer. Around 5 g of lauric acid and 0.5 g of Pd-PVP@ZIF-8 were added to the reactor. The hydrogen gas was purged three times and added to 20 bar. The reaction was carried out at a certain temperature and time. After the reaction finished, the reactor was cooled to room temperature. The gas product was released from the reactor while the liquid product was collected and weighed.

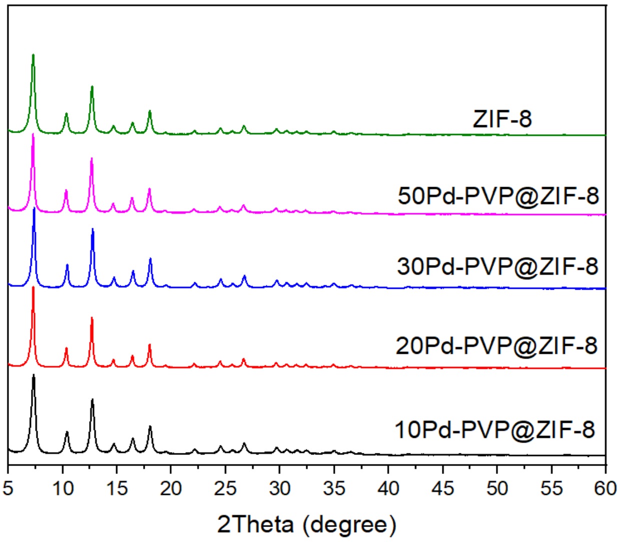

Figure 2. XRD spectra of synthesized material Pd-PVP@ZIF-8.

The liquid product was analyzed quantitively by Gas Chromatography-Mass Spectrometry (GC-MS). Before the GC-MS analysis, the 5 mL of the sample was dissolved in dichloromethane and then derivated with 50 mL N,O-Bistrifluoroacetamide. The mixture was heated at 60 °C for 10 min and injected into GC-MS. The detailed catalytic performance test is shown in Figure 1.

2.4 Catalyst Characterization

X-ray Diffraction (XRD) patterns were obtained by a Rigaku Smart Lab with the 2θ angle from 5 to 90° with a scanning rate of 5 °/min. The Brunauer-Emmett-Teller (BET) surface area, pore volume, and pore size were measured by analyzing nitrogen adsorption and desorption isotherms with Micromeritics TriStar II 3020. The Fourier Transform-Infrared Spectra (FT-IR) was collected by Bruker-Tensor II with ATR in the frequency range 4000-500 cm^{-1}. The morphology of the catalyst was observed by Scanning Electron Microscopy (SEM) on Hitachi SU-3500 equipped with Energy Dispersive X–ray Spectroscopy (EDS). Transmission electron microscopy (TEM) of the catalyst was observed using the Tecnai G2 20S-Twin Function.

3. Result and Discussion

3.1 Characterization of Pd-PVP@ZIF-8

A series of Pd-PVP@ZIF-8 was synthesized by varying the concentration of Pd-PVP solution in the synthesized solution. Figure 2 shows the XRD pattern of synthesized Pd-PVP@ZIF-8 which has a high crystallinity. The sharp and vigorous XRD peaks of all the synthesized materials are identical with ZIF-8, confirming that the introduction of Pd-PVP did not affect ZIF-8 formation. In addition, there are no obvious diffraction peaks of Pd NPs at 40° are detected in the Pd-PVP@ZIF-8, even after the addition of the highest concentration of Pd-PVP solution. It might be due to the low concentration of Pd NPs in ZIF-8.

FT-IR spectrum in Figure 3 confirms the addition of Pd-PVP solution did not change the chemical structure of ZIF-8. The synthesized 50Pd-PVP@ZIF-8 shows specific peaks of the ZIF-8 chemical structure. In ZIF-8, the stretching frequencies from 1100-1300 cm^{-1} are assigned to C−H vibration, while the vibration peaks at 1424 and 1454 cm^{-1} are assigned to C=N stretching vibration [17]. Besides having a specific peak of ZIF-8, 50Pd-PVP@ZIF-8 shows a strong vibration peak around 1661 cm^{-1} which corresponds to C=O of PVP compound.

The physical properties of synthesized materials obtained by N_2 physisorption analysis are shown in Table 1. The ZIF-8 exhibited a large surface area of around 892.07 m^2/g. The synthesized Pd-PVP@ZIF-8 was found to have a lower surface area than pure ZIF-8. The lowest surface area 636.27 m^2/g was found in 50Pd-PVP@ZIF-8 where Pd-PVP solution was added at a high concentration. The decrease in surface area was probably due to the blockage of small pores by Pd-nps [18]. The pore volume and pore size of synthesized Pd-PVP@ZIF-8 were also reduced as a consequence of the addition of Pd-PVP solution during synthesis.

Figure 4 shows the nitrogen adsorption and desorption isotherms of Pd-PVP series materials. The ZIF-8 exhibits a type IV isotherms with hysteresis suggesting a microporous-mesoporous of ZIF-8. The addition of Pd-PVP in various concentrations didn't change the type of isotherm. However, the hysteresis area was observed to decrease with an increasing amount of Pd-PVP solution.

Figure 5(a) shows the TEM image of 50Pd-PVP@ZIF-8 has a dark spot that disperses thoroughly on the surface. The dark spots appeared gathered in some areas, which means the Pd agglomerated on the surface of ZIF-8. However, it confirms that Pd-nps distributes widely on the surface of ZIF-8. The SEM-EDX was used to confirm the composition of each element on synthesized materials (Figure 5(b)). The EDX spectrums of 50Pd-PVP@ZIF-8 confirm the presence of Zn, N, C, and O which is a constituent component of ZIF-67, and Pd-nps. The Pd-nps was detected around 1 wt% with other compositions coming from chemical constituents of ZIF-8. The SEM images in Figure 5(c-d) show that the morphology of 50Pd-PVP@ZIF-8 is shaped like irregular pebbles with an uneven surface. SEM-EDX mapping elements confirm that each constituent element is well distributed (Figure 5(e-j)).

3.2 Catalytic Performance

The hydroconversion reaction of lauric acid was examined under several synthesized catalysts. The lauric acid was reacted without any solvent in a high-pressure and temperature reactor in hydrogen condition with the addition of

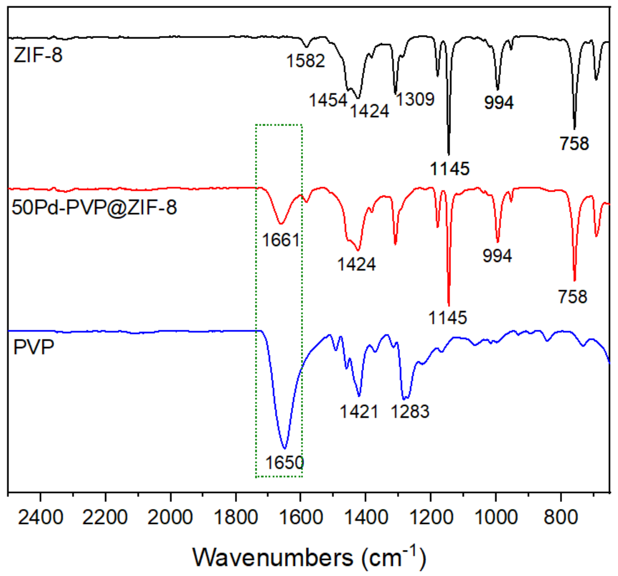

Figure 3. FT-IR spectra of synthesized material Pd-PVP@ZIF-8.

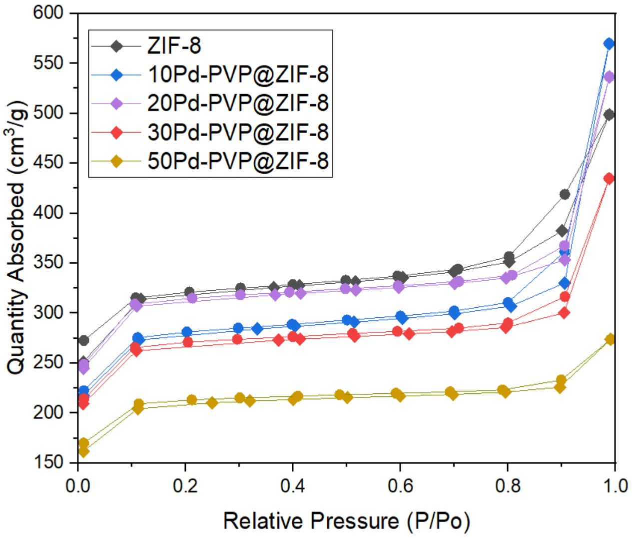

Figure 4. N_2 adsorption-desorption isotherm of synthesized ZIF materials.

Table 1. Physical properties of synthesized materials.

Catalyst	Surface Area (m^2/g)	Pore Volume (cm^3/g)	Average Pore size (nm)
ZIF-8	892.07	0.323	11.32
10Pd-PVP@ZIF-8	817.64	0.497	16.96
20Pd-PVP@ZIF-8	868.15	0.388	14.99
30Pd-PVP@ZIF-8	736.47	0.293	12.71
50Pd-PVP@ZIF-8	636.27	0.120	7.74

10 wt% of catalyst. Table 2 shows the catalytic activity of MOF-based catalysts in lauric acid conversion. It was shown that ZIF-8 exhibited a catalytic activity in lauric acid conversion to 30.6 % to produce 1-dodecanol and dodecane with selectivity of 12.9% and 2.8%, respectively. ZIF-8 consists of a Lewis acid site on Zn as well as a Lewis base on the organic linker, 2-Methylimidazole, which can support the catalytic performance of hydroconversion of lauric acid. As seen in Scheme 1, lauric acid can transform into dodecanol, which is then dehydrated to dodecene and yields dodecane. 1-Dodecanol can also react with lauric acid by esterification reaction to give dodecyl dodecanoate. Furthermore, the carboxylation or carbonylation reaction also proceeded to produce undecane during the process, which has a lower carbon content than lauric acid.

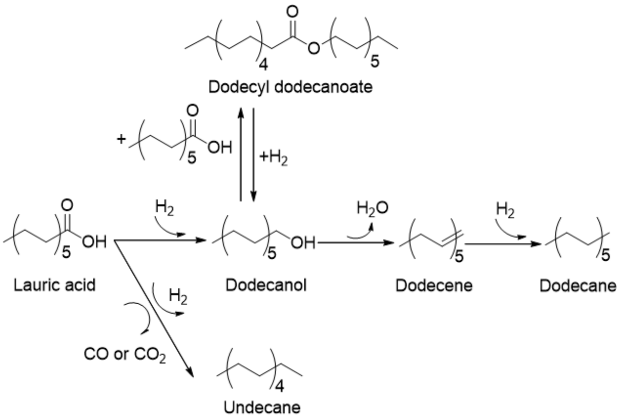

Scheme 1. Reaction pathway of lauric acid conversion to produce alcohol, ester, and alkane compound.

Loading of Pd NPs into ZIF-8 has significantly increased the conversion of lauric acid. It was found the selectivity of 1-dodecanol and dodecane was 12.9% and 2.8%, respectively (Table 2). Pd NPs exhibited to effect in improving the catalytic process. It was also reported by Takeda *et al.* [3] that the addition of Pd enhanced the catalytic activity of hydrogenation of stearic acid and improved the selectivity of 1-octadecanol compared to the addition of other noble metals including Ru, Rh, and Pt. Moreover, interestingly, when the reaction used 50Pd-PVP@ZIF-8 as a catalyst, lauric acid was converted at 87.5% with increased selectivity of 1-Dodecanol and dodecane to 77.4 % and 8.5%, respectively. The presence of Pd NPs on ZIF-8 was supported by SEM-EDX spectrum and mapping, which was well distributed on the catalyst.

Zhao *et al.* [19] reported the hybridization of metal nanoparticles with Metal-Organic Frameworks could enhance the catalytic activity through the synergy of the MOF shell and the metals. Figure 6 shows that lauric acid was

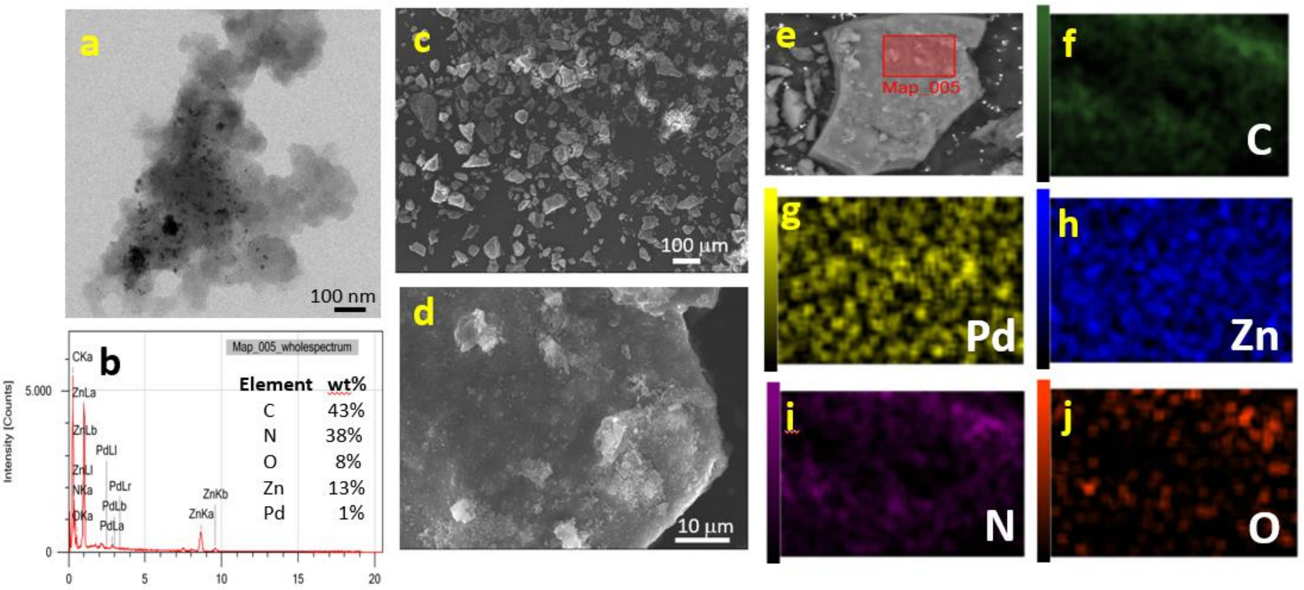

Figure 5. TEM and SEM-EDX of 50Pd-PVP@ZIF-8.

Table 2. Metal-Organic Frameworks-based catalyst for hydroconversion of lauric acid at 320 °C, 4 h, 20 bar H_2.

Catalyst	Conversion	% Selectivity	
		1-Dodecanol	Dodecane
ZIF-8	30.6	12.9	2.8
50Pd-PVP@ZIF-8	87.5	77.4	8.5

converted significantly with the increase of Pd-PVP solution. The selectivity of 1-dodecanol was enhanced by the loading of 10 to 50 mL Pd-PVP solution. It was observed that 50Pd-PVP@ZIF-8 could convert lauric acid to 87.5% and exhibited the highest selectivity among others, reaching around 77.4%. Other products, including undecane, dodecene, and dodecane remained stable at low concentrations with increasing Pd-PVP solution. The ester product, dodecyl dodecanoate was noticed to decrease along with decreasing concentration with the Pd-PVP solution. It might be due to the higher concentration of Pd-PVP can accelerate the conversion of lauric acid to dodecanol. A low concentration of lauric acid in the solution would limit the formation of dodecyl dodecanoate.

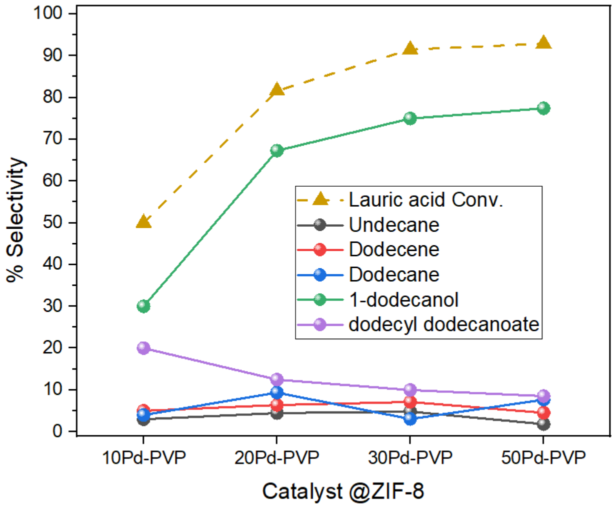

Figure 6. Effect of different loading of Pd-PVP on ZIF-8 of hydroconversion of lauric acid. Reaction condition: lauric acid 5 g, catalyst 0.5 g, 320 °C, 4 h, 20 bar H_2.

Figure 7 shows the time reaction effect using 50Pd-PVP@ZIF-8 as a catalyst for the hydroconversion of lauric acid. The conversion of lauric acid was increased with the prolongation of reaction time. At 4 h of reaction, the lauric acid was converted around 87.5%, then increased to 98.6 % and 98.9 % when reaction was exceeded to 6 h and 10 h reaction time, respectively. In addition, the selectivity of 1-dodecanol and dodecane increased to 78.2% for 6 h and 79.3% for 10 h extending reaction time, explaining that the lauric acid converted to 1-dodecanol then yields dodecane. The selectivity of dodecyl dedecanoate was known to decrease with reaction time, which means that dodecyl dodecanoate decomposes to produce 1-dodecanol as described in Scheme 1. Here, we concluded that the reaction time of 6 h was the optimum time to convert lauric acid.

The effect of lauric acid conversion with the selectivity product when the temperature was increased from 320 °C to 350 °C is shown in Figure 8. It was found the lauric acid was converted around 99% at 350 °C for hours reaction. The selectivity of 1-dodecanol decreased dramatically in contrast to the increased selectivity of dodecane. It is clear that at a higher temperature, the reaction effectively produced dodecane, in which 1-dodecanol was transformed into dodecene and then dodecane. In addition, the dodecyl dodecanoate was minimized to produce at higher temperatures. We confirmed that the temperature 320 °C was optimum to produce 1-dodecanol.

The BET analysis confirmed that 50Pd-PVP@ZIF-8 had the lowest surface area among other catalysts. However, it shows better catalytic activity to produce 1-dodecanol. This confirms that surface area had an insignificant effect on the reaction. The high activity of the catalyst was

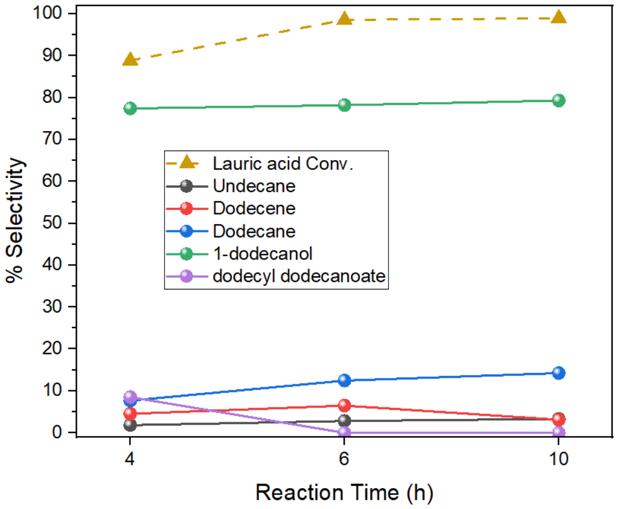

Figure 7. Effect of time reaction of hydroconversion of lauric acid using 50Pd-PVP@ZIF-8. Reaction condition: lauric acid 5 g, catalyst 0.5 g, 320 °C, 20 bar H_2.

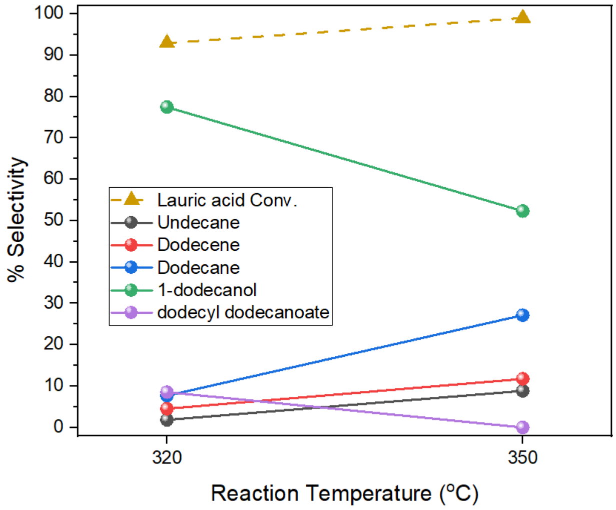

Figure 8. Effect of reaction temperature of hydroconversion of lauric acid using 50Pd-PVP@ZIF-8. Reaction condition: lauric acid 5 g, catalyst 0.5 g, 4 h, 20 bar H_2.

obtained might due to the high dispersion of Pd particles as shown in TEM images. In addition, the synergy between noble metals and the support could enhance the performance of the catalyst to convert lauric acid to 1-dodecanol. The catalytic activity of the catalyst for hydroconversion of fatty acid to fatty alcohol has been reported to have excellent performance due to the existence of oxygen vacancies on the metal-support surface that could adsorb the carbonyl oxygen and activate the C=O bond [20]. In addition, the noble metal plays a role in the dissociation of H_2 to give hydrogen atoms [21]. As well as reported reference, the Pd-PVP@ZIF-8 has metal support which facilitates activating the C=O bond of lauric acid and Pd-PVP contributes to the dissociation of hydrogen.

4. Conclusion

In summary, a Pd-PVP@ZIF-8 has been synthesized by the assembling method of Pd-PVP and ZIF-8. XRD analysis of Pd-PVP@ZIF-8 confirmed the crystalline peaks were identical with ZIF-8. The addition of Pd-PVP on the ZIF-8 didn't change the chemical structure of ZIF-8, however, it was found the surface area, pore volume, and pore size decreased due to the blockage of small pores by Pd-nps. A Pd-PVP@ZIF-8 showed catalytic activity towards hydroconversion of lauric acid to 1-dodecanol. Loading of Pd-PVP into ZIF-8 led to a large increase in catalytic activity. Among a synthesized catalyzed, a 50Pd-PVP@ZIF-8 catalyst exhibited high catalytic activity converting 98.6% lauric acid yields 78.2% of 1-dodecanol under optimum condition at 320 °C for 6 h of 20 bar hydrogen. The synergy between Pd-PVP-nps as noble metals and ZIF-8 as metal and support as well as the high dispersion of Pd particles could enhance performance in the conversion of lauric acid.

Acknowledgments

This work was supported by National Priority Program of Engineering Science (PN-IPT) LIPI 2021 and Rumah Program Research Organization of Nanotechnology and Material BRIN 2022. The authors also acknowledge the facilities, scientific, and technical support from Advanced Characterization Laboratories Serpong, National Research and Innovation Agency through E-Layanan Sains.

CRediT Author Statement

Deliana Dahnum: Investigation, Writing – review & editing, Funding acquisition; *Holanda Ramadhita*: Writing – original draft; *Andreas Andreas*: Formal analysis, Data curation; *Joni Prasetyo*: Writing-review& editing; *Aditia Nur Bakti*: Data curation, Funding acquisition; *Huyen Tran Dang*: Writing – review & editing. All authors have read and agreed to the published version of the manuscript.

References

[1] Hongloi, N., Prapainainar, P., Prapainainar, C. (2022). Review of green diesel production from fatty acid deoxygenation over Ni-based catalysts. *Molecular Catalysis*, 523, 111696. DOI: 10.1016/j.mcat.2021.111696.

[2] Canos, A.C., Iborra, S., Velty, A. (2007). Chemical routes for the transformation of biomass into chemicals. *Chemical Reviews*, 107(6), 2411–2502. DOI: 10.1021/cr050989d.

[3] Takeda, Y., Nakagawa, Y., Tomishige, K. (2012). Selective hydrogenation of higher saturated carboxylic acids to alcohols using a ReOx–Pd/SiO_2 catalyst. *Catalysis Science & Technology*, 2(11), 2221–2223. DOI: 10.1039/C2CY20302B.

[4] Lestari, S., Mäki-Arvela, P., Beltramini, J., Lu, G.Q.M., Murzin, D.Y. (2009). Transforming triglycerides and fatty acids into biofuels. *ChemSusChem*, 2(12), 1109–1119. DOI: 10.1002/cssc.200900107.

[5] Zhou, Y., Remón, J., Jiang, Z., Matharu, A.S., Hu, C. (2023). Tuning the selectivity of natural oils and fatty acids/esters deoxygenation to biofuels and fatty alcohols: A review. *Green Energy and Environment*, 8(3), 722–743. DOI: 10.1016/j.gee.2022.03.001.

[6] Manyar, H.G., Paun, C., Pilus, R., Rooney, D.W., Thompson, J.M., Hardacre, C. (2010). Highly selective and efficient hydrogenation of carboxylic acids to alcohols using titania supported Pt catalysts. *Chemical Communications*, 46(34), 6279–6281. DOI: 10.1039/c0cc01365j.

[7] Fonseca Benítez, C.A., Mazzieri, V.A., Sánchez, M.A., Benitez, V.M., Pieck, C.L. (2019). Selective hydrogenation of oleic acid to fatty alcohols on Rh-Sn-B/Al_2O_3 catalysts. Influence of Sn content. *Applied Catalysis A: General*, 584, 117149. DOI: 10.1016/j.apcata.2019.117149.

[8] Rodina, V.O., Ermakov, D.Y., Saraev, A.A., Reshetnikov, S.I., Yakovlev, V.A. (2017). Influence of reaction conditions and kinetic analysis of the selective hydrogenation of oleic acid toward fatty alcohols on Ru-Sn-B/Al_2O_3 in the flow reactor. *Applied Catalysis B: Environmental*, 209, 611–620. DOI: 10.1016/j.apcatb.2017.03.012.

[9] Takeda, Y., Tamura, M., Nakagawa, Y., Okumura, K., Tomishige, K. (2015). Characterization of Re-Pd/SiO_2 Catalysts for Hydrogenation of Stearic Acid. *ACS Catalysis*, 5 (11), 7034–7047. DOI: 10.1021/acscatal.5b01054.

[10] Guo, Z., Zhou, F., Wang, H., Liu, X., Xu, G., Zhang, Y., Fu, Y. (2019). Highly selective conversion of natural oil to alcohols or alkanes over a Pd stabilized CuZnAl catalyst under mild conditions. *Green Chemistry*, 21(18), 5046–5052. DOI: 10.1039/c9gc02379h.

[11] Wang, F., Yu, S., Xu, H., Feng, J., Guo, F., Jiang, X., Jiang, J. (2023). Selective hydrogenation of oleic acid over Flower-like Ni-Fe/SiO_2-ZrO_2 catalyst to produce fatty alcohol: Effect of SiO_2. *Fuel*, 345, 1–9. DOI: 10.1016/j.fuel.2023.128170.

[12] Sadakiyo, M., Kon-No, M., Sato, K., Nagaoka, K., Kasai, H., Kato, K., Yamauchi, M. (2014). Synthesis and catalytic application of PVP-coated Ru nanoparticles embedded in a porous metal-organic framework. *Dalton Transactions*, 43(29), 11295–11298. DOI: 10.1039/c4dt00996g.

[13] Song, X., Guan, Q., Cheng, Z., Li, W. (2018). Eco-friendly controllable synthesis of highly dispersed ZIF-8 embedded in porous Al_2O_3 and its hydrogenation properties after encapsulating Pt nanoparticles. *Applied Catalysis B: Environmental*, 227, 13–23. DOI: 10.1016/j.apcatb.2018.01.022.

[14] Van Lent, R., Auras, S.V., Cao, K., Walsh, A.J., Gleeson, M.A., Juurlink, L.B.F. (2019). Site-specific reactivity of molecules with surface defects—the case of H_2 dissociation on Pt. *Science*, 363(6423), 155–157. DOI: 10.1126/science.aau6716.

[15] Liu, J., He, J., Wang, L., Li, R., Chen, P., Rao, X., Deng, L., Rong, L., Lei, J. (2016). NiO-PTA supported on ZIF-8 as a highly effective catalyst for hydrocracking of Jatropha oil. *Scientific Reports*, 6, 23667. DOI: 10.1038/srep23667.

[16] Jiang, H., Yan, Q., Chen, R.Z., Xing, W.H. (2016). Synthesis of Pd@ZIF-8 via an assembly method: Influence of the molar ratios of Pd/Zn^{2+} and 2-methylimidazole/Zn^{2+}. *Microporous and Mesoporous Materials*, 225, 33–40. DOI: 10.1016/j.micromeso.2015.12.010.

[17] Nagarjun, N., Dhakshinamoorthy, A. (2019). A Cu-Doped ZIF-8 metal organic framework as a heterogeneous solid catalyst for aerobic oxidation of benzylic hydrocarbons. *New Journal of Chemistry*, 43 (47), 18702–18712. DOI: 10.1039/c9nj03698a.

[18] Regali, F., Liotta, L.F., Venezia, A.M., Montes, V., Boutonnet, M., Järås, S. (2014). Effect of metal loading on activity, selectivity and deactivation behavior of Pd/silica-alumina catalysts in the hydroconversion of n-hexadecane. *Catalysis Today*, 223, 87–96. DOI: 10.1016/j.cattod.2013.08.028.

[19] Zhao, Y., Ni, X., Ye, S., Gu, Z. G., Li, Y., Ngai, T. (2020). A Smart Route for Encapsulating Pd Nanoparticles into a ZIF-8 Hollow Microsphere and Their Superior Catalytic Properties. *Langmuir*, 36 (8), 2037–2043. DOI: 10.1021/acs.langmuir.9b03731.

[20] Yue, S., Ding, X., Liu, X., Guo, Y., Wang, Y. (2022). High-efficient production of fatty alcohol via hydrogenation of fatty acid over Cu-NbOx/SBA-15 catalyst. *Catalysis Today*, *405*–406, 221–226. DOI: 10.1016/j.cattod.2022.05.021.

[21] Kon, K., Toyao, T., Onodera, W., Siddiki, S.M.A.H., Shimizu, K.I. (2017). Hydrodeoxygenation of Fatty Acids, Triglycerides, and Ketones to Liquid Alkanes by a Pt–MoOx/TiO_2 Catalyst. *ChemCatChem*, 9(14), 2822–2827. DOI: 10.1002/cctc.201700219.